# Particle-Swarm-Optimization-Based Nonintrusive Demand Monitoring and Load Identification in Smart Meters

Hsueh-Hsien Chang, *Member, IEEE*, Lung-Shu Lin, Nanming Chen, and Wei-Jen Lee, *Fellow, IEEE*

***Abstract*—Compared with the traditional load monitoring system, a nonintrusive load monitoring (NILM) system is simple to install and does not need an individual sensor for each load. Accordingly, the NILM system can be applied for wide load monitoring and become a powerful energy management and measurement system. Although several NILM algorithms have been developed during the last two decades, recognition accuracy and computational efficiency remain as challenges. To minimize training time and improve recognition accuracy, particle swarm optimization is adopted in this paper to optimize parameters of training algorithms in artificial neural networks. The proposed algorithm is verified through the combination of Electromagnetic Transients Program simulations and field measurements. The results indicate that the proposed method significantly improves recognition accuracy and computational efficiency under multiple operation conditions.**

***Index Terms*—Artificial neural networks (ANNs), nonintrusive load monitoring (NILM), particle swarm optimization (PSO), smart meters.**

## I. Introduction

AS ESTIMATED at the end of 2009, the global reserves-to-production ratio of oil, natural gas, and coal is 45.7, 62.8, and 119 years, respectively [1]. Currently, oil and natural gas are still the main energy sources. The annual growth rate of energy consumption on oil and natural gas is around 2.3% and 2.2% [2]. With the current rate of increase, these natural resources will not be able to meet the demand after the middle of the twenty-first century.

The deployment of advanced metering infrastructure (AMI) is viewed as a building block of smart grids. The AMI system includes smart meters, communication infrastructure, and Meter Database Management System (MDMS). Smart meters can provide information such as real-time energy consumption, maximum demand, consumption pattern, and power quality. Utilities can use AMI to provide results of analyses and offer incentive programs to encourage the user to adjust the consumption pattern or replace more efficient electrical appliances to promote energy efficiency. In addition, collection of energy consumption data from all clients based on a regular basis allows utility companies to efficiently manage electricity demands and establish a future expansion plan. Fig. 1 illustrates the architecture of smart meters in an AMI system.

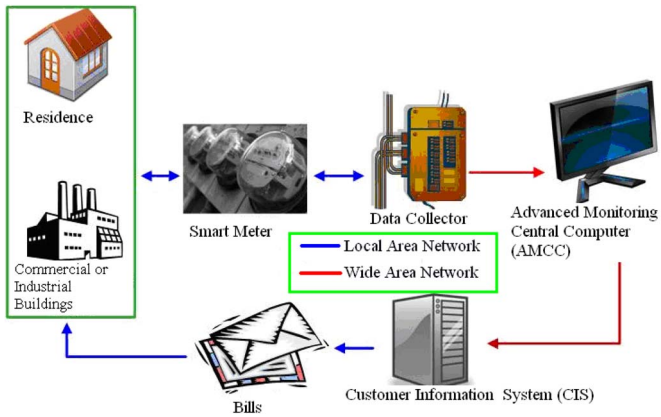


Fig. 1. Smart meter in an AMI system.

Traditional load monitoring instrumentation systems use meters to monitor each individual load because they tend to be comprehensive. These meters may incur redundant time and costs to install and maintain. Furthermore, increasing numbers of meters may influence system reliability. Some researches also indicate that the utilization of load monitoring systems has been questioned by load monitoring system practitioners. Instead of following the traditional approach, a nonintrusive load monitoring (NILM) system is the trend for future development [3], [4]. It can be easily installed with lower cost. With a proper algorithm, the NILM system can identify various loads and the status of loads, including electric power demands, type of appliances, time of use, overload capacities of loads, etc. Future load monitoring systems should focus on developing strategies to minimize the number of instruments and improve recognition accuracy.

Due to the importance of accurate power signature recognition in an NILM process, many researchers have devoted

Manuscript received June 29, 2012; revised November 29, 2012; accepted December 14, 2012. Date of publication April 18, 2013; date of current version September 16, 2013. Paper 2012-ESC-228.R1, presented at the 2012 IEEE Industry Applications Society Annual Meeting, Las Vegas, NV, USA, October 7–11, and approved for publication in the IEEE Transactions on Industry Applications by the Energy Systems Committee of the IEEE Industry Applications Society. This work was supported by the National Science Council, Taiwan, under Contract NSC 101-2221-E-228-001.

H.-H. Chang is with Jinwen University of Science and Technology, New Taipei 23154, Taiwan (e-mail: sschang@just.edu.tw).

L.-S. Lin is with Chung-Shan Institute of Science and Technology, Taoyuan 325, Taiwan (e-mail: rhlin0605@gmail.com).

N. Chen is with National Taiwan University of Science and Technology, Taipei 106, Taiwan (e-mail: nmchen@ee.ntust.edu.tw).

W.-J. Lee is with the Energy Systems Research Center, University of Texas at Arlington, Arlington, TX 76019 USA (e-mail: wlee@uta.edu).

Color versions of one or more of the figures in this paper are available online at http://ieeexplore.ieee.org.

Digital Object Identifier 10.1109/TIA.2013.2258875

their efforts in this area and reported their findings in articles. Hart [3] proposed a load identification method that monitors the steady-state behavior of loads. Hart conceptualized a finite-state machine to represent a single appliance in which power consumption discretely varies with each step change. Although this method performs well in the sample appliance, it cannot monitor small appliances or appliances that are always on or have nondiscrete changes in power [3], [5]. Cole and Albicki [6], [7] presented a data extraction method and a steady-state load identification algorithm for NILM. This algorithm can be used for load switching between individual appliances when one or more appliances are switched on or off. However, it requires an extended period of time to accumulate real power (P) and reactive power (Q) data and cannot recognize any appliance power consumption that does not change [7]. Chang *et al.* [8] employed a turn-on transient energy algorithm to classify several unknown transient behaviors for load identification. This algorithm, however, is complex since it requires a high sampling rate to detect the transient behavior of the loads. In addition, the detection of transient behavior can only be applied into the simultaneous transient of multiple loads.

Several recent studies have proposed new power signature analyses [9]–[11], load identification methods [12]–[15], and feature selection approaches [16]–[18] to recognize loads and solve classification problems. For the load identification methods, many papers have been published to improve the performance of recognition using artificial neural networks (ANNs) for the NILM system. For example, Srinivasan *et al.* [15] proposed a neural-network-based approach to identify a nonintrusive harmonic source. However, the method does not incorporate the various operational modes of each load and operation under different voltage sources.

Some researchers have undertaken to find sets of weights of ANNs by using a genetic algorithm (GA), but migration among subspecies of machines will be a problem due to GA crossover. In the past several years, particle swarm optimization (PSO) has been successfully applied to many applications. It is demonstrated that PSO has potential to obtain better results faster with the requirement of fewer parameters [19]. To mitigate the disadvantages of the previously published research, a new method for load identification of the NILM system is proposed in this paper. This method applies PSO to optimize the parameters of training algorithms in ANNs and to find the optimum solution of load pattern recognition for traditional steady-state power signatures. Accordingly, the proposed method can improve recognition accuracy and reduce computational requirements in NILM. The proposed technique is robust to operational modes, voltage variations, and power consumption changes. In addition to residential loads, the proposed method can be also applied for commercial and industrial loads. Moreover, the proposed method can identify multiple loads with simultaneous starting time.

Fig. 2 shows the overall scheme of the proposed NILM system. Single-phase two-wire and single-phase three-wire systems are used to represent a typical residential system. An MDMS connects to the smart meter with the embedded NILM system to manage and recognize the operation status, power quality, and power consumption patterns through a wireless network. The client computers can also read all the information from the MDMS through Internet or Web systems.

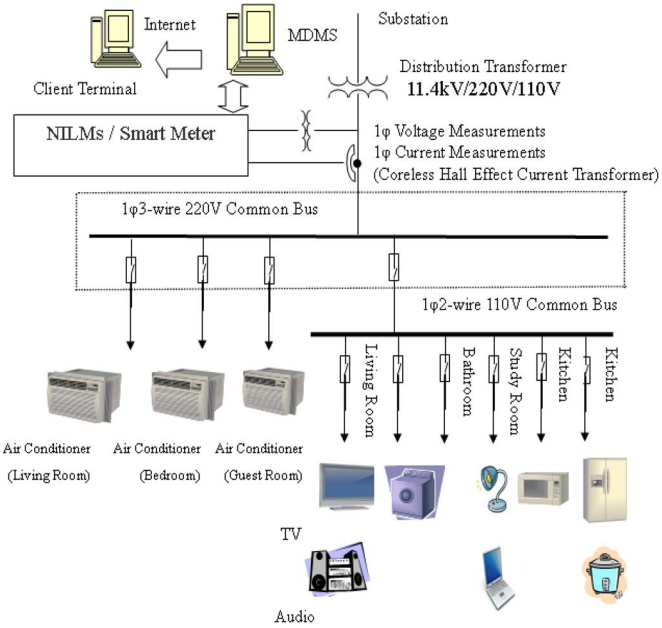


Fig. 2. Smart meter and load identification system for an NILM system.

## II. Data Acquisition and Data Preprocessing

The main parameters to be acquired are the voltage and current of aggregated loads. Representative samples of the loads are monitored for training purposes. A sampling rate of 100 points per cycle is sufficient for the application. Therefore, the sampling frequency is set at 6 kHz.

For steady-state linear time-invariant loads, complex power can be calculated from voltage, current, and phase angles. In (2), the real part of complex power (S) is real power (P) or average power, and the imaginary part is reactive power (Q). They can be computed by

$$V = V_m e^{j\theta_V} \qquad I = I_m e^{j\theta_I} \tag{1}$$

$$S = \frac{1}{2} V \bar{I} = \frac{1}{2} V_m I_m e^{j(\theta_V - \theta_I)} = P + jQ \tag{2}$$

where variables $V_m$ and $I_m$ are the maximum values of voltage and current, and variables $\theta_V$ and $\theta_I$ are the phase angles of voltage and current.

The current and voltage consumed for a periodically nonlinear load can be represented by a Fourier series expansion. The appropriate coefficients corresponding to the current and voltage in each harmonic are extracted from the results. The number of terms represented by the expansion determines the dimension of the feature vector. Real power and reactive power can be computed by

$$I_n = Z_n^{-1} V_n = Y_n V_n \tag{3}$$

$$P = \sum_{n=0}^{N} P_n = P_0 + \sum_{n=1}^{N} P_n$$

$$= V_0 I_0 + \sum_{n=1}^{N} V_n I_n \cos(\theta_{V_n} - \theta_{I_n}) \tag{4}$$

$$Q = \sum_{n=1}^{N} Q_n = \sum_{n=1}^{N} V_n I_n \sin(\theta_{V_n} - \theta_{I_n}) \tag{5}$$

where $n$ is the frequency number, $n = 0, 1, 2, \ldots, N$; $Z_n$ and $Y_n$ are the impedance matrix and the admittance matrix of the system, respectively; $V_0$ and $I_0$ are the dc voltage and current, respectively; $V_n$ and $I_n$ are the effective $n$th harmonic components of the voltage and current; and $\theta_{V_n}$ and $\theta_{I_n}$ represent the $n$th harmonic components of the voltage and current phase angles, respectively. With a 6-K/s sampling rate, it gives us additional information for load identification. For example, transient energy $(U_T)$ can be used to enhance the capability of load identification when different load combinations yield the same real power and reactive power [8]. Unless they have identical transient energy, they are distinguishable. The possibility of using harmonic current signatures for load identification is also explored. However, it requires further investigation since the current harmonic contents are also affected by the voltage source.

Neural network training can be made more efficient if certain preprocessing steps are performed on the network inputs and targets [20]. Before training, it is often useful to normalize the inputs and desired outputs so that they always fall within a specified range. The approach for scaling network inputs and desired outputs is to normalize the mean and standard deviation of the training set, normalizing the inputs and desired outputs so that they will have zero mean and unity standard deviation. These can be accomplished by

$$P_n = (P - meanp)/stdp \tag{6}$$

$$t_n = (t - meant)/stdt \tag{7}$$

where matrices $\boldsymbol{P}$ and $\boldsymbol{t}$ are the original network inputs and desired outputs, respectively, and matrices $\boldsymbol{P}_n$ and $\boldsymbol{t}_n$ represent the normalized inputs and normalized desired outputs. Vectors $\boldsymbol{meanp}$ and $\boldsymbol{stdp}$ are the means and standard deviations of the original inputs, whereas vectors $\boldsymbol{meant}$ and $\boldsymbol{stdt}$ are the means and standard deviations of the desired outputs.

## III. Proposed Methods

### A. PSO

PSO is a population-based stochastic optimization technique developed by Dr. Eberhart and Dr. Kennedy in 1995 [21], simulated by social behavior of bird flocking or fish schooling. PSO shares many similarities with evolutionary computation techniques such as GA. The system is initialized with a population of random solutions and searches for optimum by updating generations. The potential solutions in PSO, which are called particles, fly through the problem space by following the current optimum particles. Each particle keeps track of its coordinates in the problem space, which are associated with the best solution, e.g., fitness, it has achieved so far. This value is called

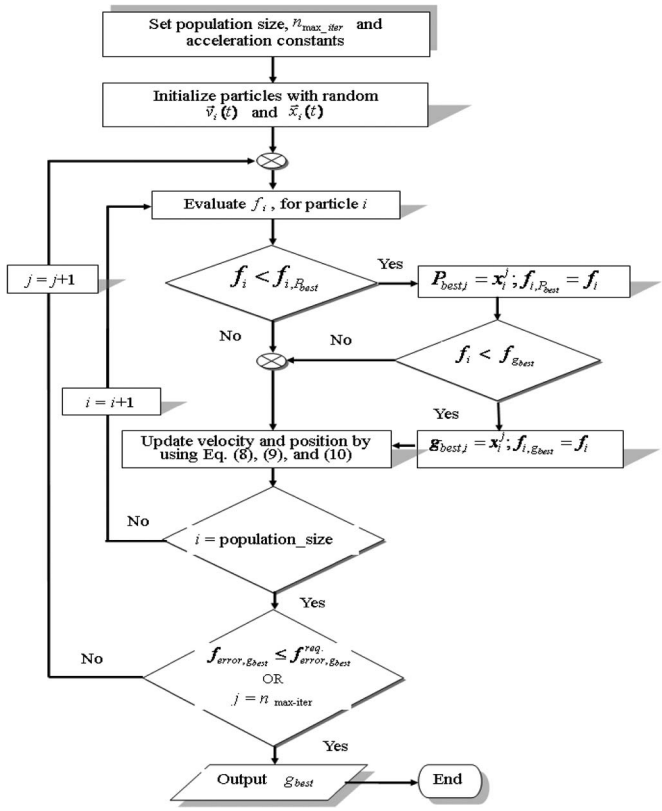


Fig. 3. Process flow of the PSO algorithm.

particle best value $(p_{\text{best}})$. Another "best" value is obtained from the best performer in the neighbors of the particle. This location is called location best value $(l_{\text{best}})$. When a particle takes all the population as its global topological neighbors, the best value is a global best and is called global best value $(g_{\text{best}})$. The PSO concept consists of each time step and accelerating of each particle toward its $p_{\text{best}}$ and $l_{\text{best}}$ $(g_{\text{best}})$ locations. Acceleration is weighted by a random term, with separate random numbers being generated for acceleration toward $p_{\text{best}}$ and $g_{\text{best}}$ locations. Fig. 3 illustrates the process flow of the proposed PSO.

The steps of the PSO algorithm are as follows.

Step 1: Set population size, the number of maximum iteration $(n_{\max\_\text{iter}})$, and acceleration constants.

Step 2: Initialize an array of particles with random positions and velocities on $N$ dimensions.

Step 3: Evaluate the desired fitness function in $N$ variables.

Step 4: Compare evaluation of the fitness function with the particle's previous best value $(f_{i,pbest})$: If the current value $(f_i)$ is smaller, the fitness value of the particle best value will be replaced by the current value, and the position of $p_{\text{best}}$ will be replaced by the current position in $N$-dimensional hyperspace; otherwise, go to step 6.

Step 5: Compare evaluation of the fitness function with the group's previous best value $(f_{gbest})$: If the current value $(f_i)$ is smaller, then the fitness value of the global best value will be replaced by the current value, and the position of $g_{\text{best}}$ will be replaced by the particle's array index; otherwise, go to step 6.

Step 6: The modification of the moving orbit of particle $i$ to update velocity and position by the following formula:

$$\vec{v}_i(t+1) = \omega\vec{v}_i(t) + c_1\vec{r}_1 \times \left(\vec{p}_{\text{best},i}(t) - \vec{x}_i(t)\right) + c_2\vec{r}_2 \times \left(\vec{g}_{\text{best}}(t) - \vec{x}_i(t)\right) \quad (8)$$

$$\vec{x}_i(t+1) = \vec{x}_i(t) + \vec{v}_i(t+1) \quad (9)$$

$$w = w_u - (w_u - w_l) \cdot (n_{\text{iter}}/n_{\max\_\text{iter}}) \quad (10)$$

where vectors $\vec{v}_i(t+1)$ and $\vec{x}_i(t+1)$ represent the new velocity and position of particle $i$ at time $t+1$, vectors $\vec{v}_i(t)$ and $\vec{x}_i(t)$ represent the original velocity and position of particle $i$ at time $t$, $\vec{p}_{\text{best},i}(t)$ and $\vec{g}_{\text{best}}(t)$ represent the position of the best solution discovered so far by particle $i$ and by all particles in the neighborhood of particle $i$, $c_1$ and $c_2$ are the acceleration constants, $\vec{r}_1$ and $\vec{r}_2$ are random vectors with each constituent drawn with a uniform probability from [0, 1], and $w$ is the inertia weight, which controls the degree that the velocity of a particle at time $t$ influences the velocity of that particle at time $t+1$. Inertia weight $w_u$ is the maximum inertia weight, and $w_l$ is the minimum inertia weight.

Loop to step 3 and repeat until a criterion of population size is met.

Loop to step 2 and repeat until a maximum iteration ($n_{\max\_\text{iter}}$) is met or until the error of the group's best fitness ($f_{\text{error},g_{\text{best}}}$) is smaller than or equal to the required error of the group's best fitness ($f^{\text{req.}}_{\text{error},g_{\text{best}}}$).

### B. ANNs

Pattern classifiers partition a multidimensional space into decision regions that indicate the class to which any input belongs [9].

*1) Training Algorithms and Fitness Function:* Overfitting is a typical problem that occurs during ANN training. Bayesian regularization mean square error (MSE) typically provides better generalization performance than early stopping because Bayesian regularization does not require a validation data set to be separated from the training data set. In other words, the input training data use all training data sets. This advantage is particularly important when the data set is small.

The typical fitness function used for training a feedforward neural network is the mean sum of squares of network errors, also called MSE, which is the average squared error between network outputs and desired outputs. Thus

$$f(l) = \text{MSE}(l) = E(l) = \frac{1}{2}\sum_{j\in C}(t_j(l) - a_j(l))^2 \quad (11)$$

where variable $t_j(l)$ is the desired output for the $l$th iteration at node $j$, and variable $a_j(l)$ is the network output for the $l$th iteration at node $j$.

*2) MFNN:* Most backpropagation ANN (BP-ANN) applications utilize single- or multilayer perceptron networks by using gradient-descent training methods combined with learning via backpropagation. These multilayer perceptrons can be trained under supervision using analytical functions to activate network nodes ("neurons") and by applying a backward error-propagation algorithm and optimization methods (e.g., PSO or GA) to update interconnecting weights $(w_{ij})$ and thresholds $(b_j)$ until sufficient recognition capability is achieved. A trainable classifier uses the BP classifier for a multilayer feedforward neural network (MFNN) in this study. "Classification" in this context is a mapping from feature space to a set of class labels, which are the names of loads.

A supervised MFNN is generally divided into three layers, namely, input, hidden, and output layers. These neurons are connected by links with weights that are selected to meet the desired relationship between input and output neurons. The MFNN in this study is utilized to identify loads in the NILM system. The input, output, and hidden layers of the BP-ANN are as follows.

a) *Input layer*: power signature information, including real power and reactive power, for an electrical service entrance serves as inputs.
b) *Output layer*: the number of output neurons is the same as the number of individual loads identified. Each binary bit serves as a load indicator for ON/OFF status.
c) *Hidden layer*: only one hidden layer is used in this study. Some heuristics have been developed that can determine the number of neurons in a hidden layer [22]. The common number of neurons in a hidden layer is the sum of the number of neurons in an input layer and that in an output layer.

Fig. 4 presents the scheme for coding an array of particles. All weights and thresholds are used as the particles. In the example in Fig. 4, the number of input neurons is 2, the number of hidden neurons is 5, and the number of output neurons is 3. The new weights and thresholds can be updated by

$$\begin{aligned} w_{ij}(l+1) &= w_{ij}(l) + \Delta w_{ij}(l) \\ &= w_{ij}(l) + \left((-\eta)\cdot\frac{\partial E(l)}{\partial w_{ij}(l)}\right) \\ &= w_{ij}(l) + \left((-\eta)\cdot\left(-\delta_j^n(l)\right)\cdot a_i^{n-1}(l)\right) \end{aligned} \quad (12)$$

$$\begin{aligned} b_j(l+1) &= b_j(l) + \Delta b_j(l) \\ &= b_j(l) + \left((-\eta)\cdot\frac{\partial E(l)}{\partial b_j(l)}\right) \\ &= b_j(l) + \left((-\eta)\cdot\delta_j^n(l)\right) \end{aligned} \quad (13)$$

where variable $w_{ij}(l+1)$ is the new weight from node $j$ to node $i$ for the $(l+1)$th iteration; $w_{ij}(l)$ is the weight produced by PSO from node $j$ to node $i$ for the $l$th iteration; variable $\eta$ is the learning rate of network; $b_j(l+1)$ is the new threshold at node $j$ for the $(l+1)$th iteration; and $b_j(l)$ is the threshold produced by PSO at node $j$ for the $l$th iteration. $\delta_j^n(l)$ is

$$\delta_j^n(l) = \left(t_j(l) - a_j^n(l)\right)\cdot f'\left(net_j^n(l)\right) \quad (14)$$

or

$$\delta_j^n(l) = \left(\sum_k \delta_k^{n+1}(l)\cdot w_{jk}(l)\right)\cdot f'\left(net_j^n(l)\right) \quad (15)$$

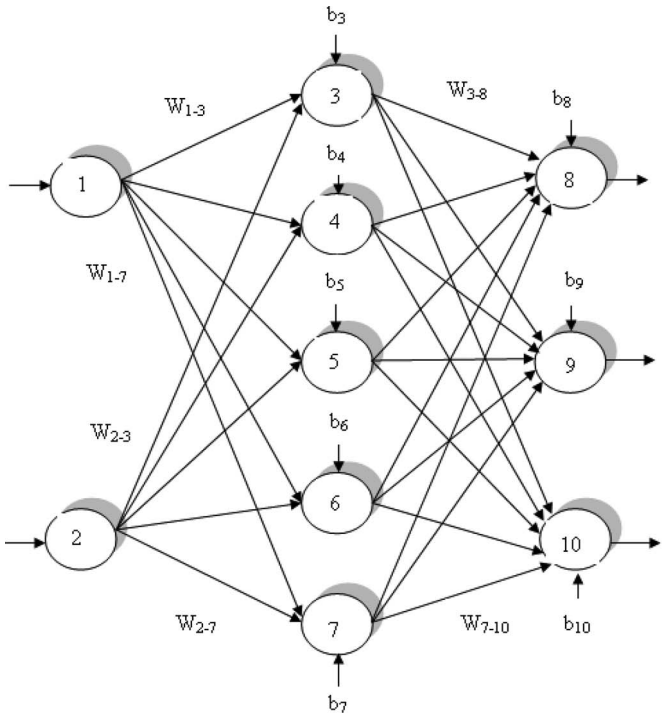


| | | | | | | | | |
|---|---|---|---|---|---|---|---|---|
| $W_{1\text{-}3}$ | … | $W_{1\text{-}7}$ | $W_{2\text{-}3}$ | … | $W_{2\text{-}7}$ | $W_{3\text{-}8}$ | … | $W_{3\text{-}10}$ |

| | | | | | | | | |
|---|---|---|---|---|---|---|---|---|
| $W_{4\text{-}8}$ | … | $W_{4\text{-}10}$ | $W_{5\text{-}8}$ | … | $W_{5\text{-}10}$ | $W_{6\text{-}8}$ | … | $W_{6\text{-}10}$ |

| | | | | | |
|---|---|---|---|---|---|
| $W_{7\text{-}8}$ | … | $W_{7\text{-}10}$ | $b_3$ | … | $b_{10}$ |

Fig. 4. Coding scheme of an array of particles.

where $f(net_j^n(l))$ is the Sigmoid activation function of the network at node $j$ of the $n$th layer for the $l$th iteration, it is

$$f\left(net_j^n(l)\right) = a_j^n(l) = \frac{1}{1+\exp^{-net_j^n(l)}} \tag{16}$$

$$net_j^n(l) = \left(\sum_i w_{ij}(l)\cdot a_i^{n-1}(l)\right) - b_j(l). \tag{17}$$

Fig. 5 shows the flowchart of NILM with the PSO algorithm in smart meters. First, data samples are measured by a data acquisition device for the voltage and current waveforms at the service entrance, and then, full input data sets of the BP-ANN are preprocessed to be the training and test data sets of PQ. Afterward, the proposed methods are applied to find the optimal outputs of the BP-ANN, to identify the loads, and finally, to display power demand analyses and the ON/OFF status of loads. The power quality indexes will be alarmed when the system is overloading.

## IV. Experimental Results

### A. Study Environment

Experimental data sets were generated by preprocessing the data on the voltage and current waveform of the total load. Each final sample consists of $(T \times 60 \times 100)$ samples obtained over a period of $T$. Each example of the power feature includes a

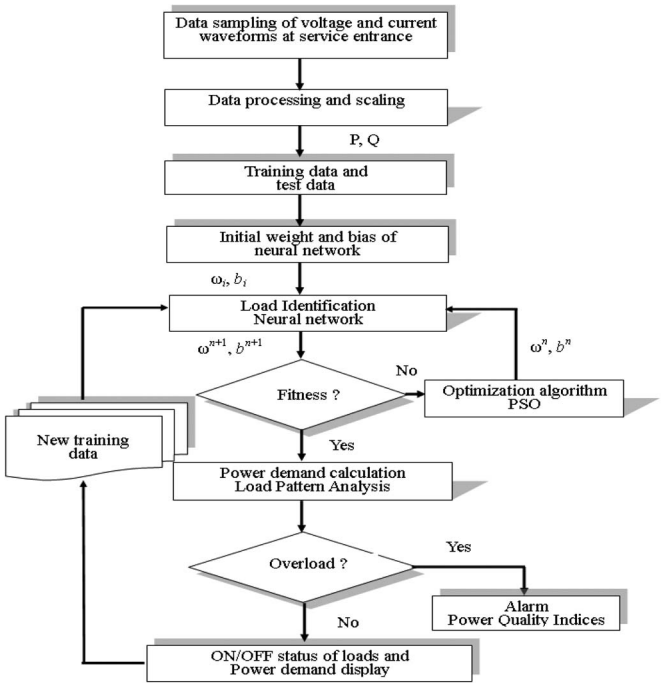


Fig. 5. Flowchart of the proposed NILM system.

voltage variation from $-5\%$ to $+5\%$ at $1\%$ intervals, yielding 11 examples of power feature for each scenario and $(2^N - 1) \times 11$ raw data for $2^N - 1$ scenarios given $N$ loads in a power system network. To confirm the inferential power of the neural networks, the full raw data set creates, respectively, a $((2^N - 1) \times 11)/2$ matrix as the training data set and test data set. The full input data set $((2^N - 1) \times 11) \times (T \times 60 \times 100)$ matrix includes the training data set and the test data set. The training data and test data are randomly selected from all data. A neural network simulation program was designed using MATLAB. The program was run to identify load on a DELL PC with an Intel 2.33-GHz Core 2 Duo central processing unit.

Each entry in the table represents ten different trials, and each trial uses random initial weights. In each case, the network is trained until the MSE is less than 0.0001 or the number of iterations reaches 1500.

### B. Results

*1) Case Study 1—EMTP Simulation:* In case study 1, a simulated NILM system constructed by the Electromagnetic Transients Program (EMTP) software program monitors the voltage and current waveforms in a three-phase electrical service entrance powering representative loads in an industrial building. The neural network algorithm in the NILM system identifies three loads of the 480-V common bus with steady-state P and Q signatures observed during operation. These loads include a 160-hp induction motor, a 123-hp induction motor driven by line frequency variable-voltage drives, and a bank of loads supplied by a six-pulse thyristor rectifier for ac power.

Table I shows that the test recognition accuracy of load in multiple operations using the proposed method (BP-ANN with PSO) reaches 99.21%; it is higher than that using BP-ANN with GA and BP-ANN without optimization.

TABLE I
RESULTS OF LOAD IDENTIFICATION IN CASE STUDY 1

| Methods | BP-ANN | GA and BP-ANN | PSO and BP-ANN |
|---|---|---|---|
| Recognition Accuracy In Training (%) | 98.97 | 100 | 100 |
| Recognition Accuracy In Test (%) | 96.84 | 98.95 | 99.21 |
| Training Time (s) | 4.13 | 3.90 | 3.32 |
| Test Time (s) | 0.007 | 0.007 | 0.007 |

TABLE II
RESULTS OF LOAD IDENTIFICATION IN CASE STUDY 2

| Methods | BP-ANN | GA and BP-ANN | PSO and BP-ANN |
|---|---|---|---|
| Recognition Accuracy In Training (%) | 94.62 | 97.95 | 100 |
| Recognition Accuracy In Test (%) | 86.05 | 91.32 | 92.90 |
| Training Time (s) | 5.27 | 6.84 | 4.67 |
| Test Time (s) | 0.007 | 0.007 | 0.007 |

In computation time, the time of training when optimization uses the PSO algorithm has much less time compared with the GA with BP-ANN and only BP-ANN.

*2) Case Study 2—Experiment:* The NILM system in case study 2 monitors the voltage and current waveforms in a three-phase electrical service entrance powering representative loads in a laboratory. The neural network algorithm in the NILM system identifies three actual loads on a 220-V common bus with steady-state signatures. These loads include a three-phase $RL$ linear load, a one-phase 0.2-hp induction motor, and a three-phase 1-hp induction motor. The real power and reactive power of the $RL$ linear load is 800 W and 500 Var, respectively.

Table II shows that the test recognition accuracy of load recognition in multiple operations of BP-ANN with PSO is 92.90%; it is also the highest among all others.

In computation requirements, the time of training when optimization uses the PSO algorithm has also less time compared with other methods.

*3) Case Study 3—Experiment on Single-Phase Three-Wire System:* In case study 3, the NILM system monitors voltage and current waveforms in a single-phase three-wire electrical service entrance powering a collection of loads representing the major load classes in a commercial or residential building. The neural network algorithm in the NILM system identifies five actual loads operating on a 220-V common bus with steady-state signatures. These loads include a 910-W air conditioner, a 100-W television, a 1200-W vacuum cleaner, a 780-W hair dryer, and a 168-W desktop computer. Fig. 6 shows the overall scheme in the NILM system for this case study.

Figs. 7–9 illustrate waveforms of power signatures at service entrance, results of the Fourier transform of current, and event records, respectively. Table III shows that values for training and test recognition accuracy of load identification in multiple operations are higher than 92% and 88% for features with steady-state PQ under with and without any optimization algorithm, respectively. However, the test recognition accuracy of load recognition in multiple operations using BP-ANN with

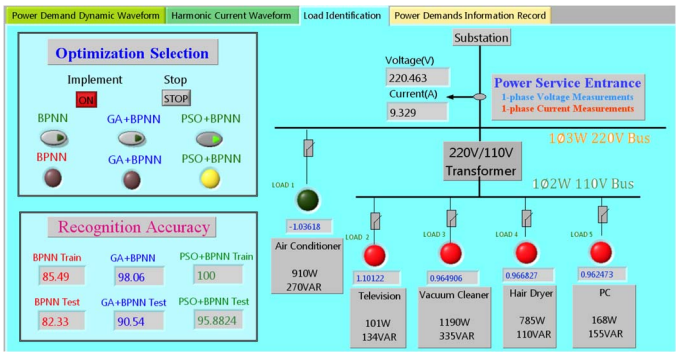


Fig. 6. NILM system of case study 3.

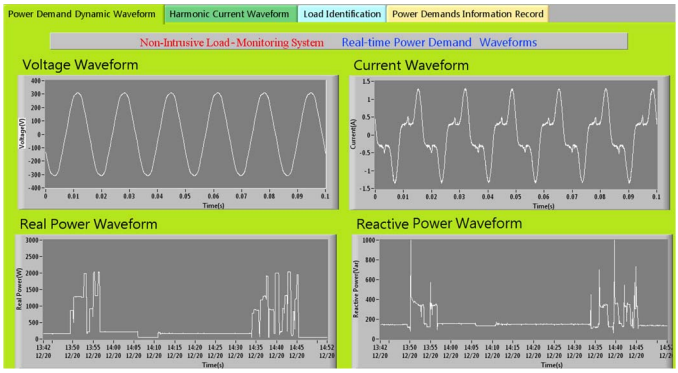


Fig. 7. Power signature waveforms in case study 3.

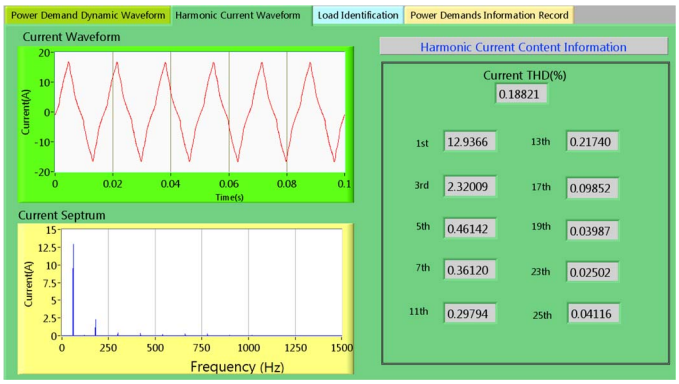


Fig. 8. Harmonic waveforms in case study 3.

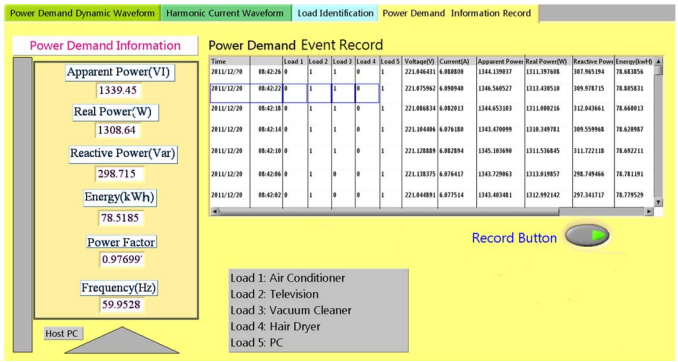


Fig. 9. Event records in case study 3.

TABLE III
RESULTS OF LOAD IDENTIFICATION IN CASE STUDY 3

| Methods | BP-ANN | GA and BP-ANN | PSO and BP-ANN |
|---|---|---|---|
| Recognition Accuracy In Training (%) | 92.69 | 96.84 | 99.88 |
| Recognition Accuracy In Test (%) | 88.30 | 94.82 | 96.65 |
| Training Time (s) | 80.28 | 107.06 | 90.32 |
| Test Time (s) | 0.010 | 0.009 | 0.008 |

PSO is 96.65%; it is higher than that using BP-ANN with GA and BP-ANN without an optimization algorithm. The training recognition accuracy of BP-ANN with PSO is near 100%.

In computation requirements, the time of training when optimization uses the PSO algorithm has less time than GA and BP-ANN, but it needs more time compared with only BP-ANN in the case study.

## V. CONCLUSION

This paper has employed PSO and BP-ANN to improve the efficiency of load identification and computational time for the NILM system. The experimental results reveal that the recognition accuracy of the proposed method for real power and reactive power is higher than that of other methods. In addition, computational time can be improved by using the proposed method. The proposed optimization technique is robust to different operational modes, voltage variations, and power consumption changes. Moreover, the proposed method can be employed in different loads with the simultaneous turn-on events of multiple loads and only one load turned on when the other loads operated in steady state.

## REFERENCES


[1] *BP Statistical Review of World Energy*, BP Global, Houston, TX, USA, Jun. 2010.

[2] Bureau of Energy, *Long-Term Demand Forecast and Energy Report*, Ministry of Econom. Affairs, Taipei, Taiwan, Jan. 2011.

[3] G. W. Hart, "Nonintrusive appliance load monitoring," *Proc. IEEE*, vol. 80, no. 12, pp. 1870–1891, Dec. 1992.

[4] S. B. Leeb, "A conjoint pattern recognition approach to nonintrusive load monitoring," Ph.D. dissertation, Dept. Elect. Eng. Comput. Sci., Massachusetts Inst. Technol., Cambridge, MA, USA, 1993.

[5] A. I. Cole and A. Albicki, "Nonintrusive identification of electrical loads in a three-phase environment based on harmonic content," in *Proc. IEEE Instrum. Meas. Technol. Conf.*, 2000, pp. 24–29.

[6] A. I. Cole and A. Albicki, "Data extraction for effective non-intrusive identification of residential power loads," in *Proc. IEEE Instrum. Meas. Technol. Conf.*, 1998, pp. 812–815.

[7] A. I. Cole and A. Albicki, "Algorithm for non-intrusive identification of residential appliances," in *Proc. IEEE Int. Symp. Circuits Syst.*, 1998, pp. 338–341.

[8] H. H. Chang, K. L. Chen, Y. P. Tsai, and W. J. Lee, "A new measurement method for power signatures of non-intrusive demand monitoring and load identification," *IEEE Trans. Ind. Appl.*, vol. 48, no. 2, pp. 764–771, Mar./Apr. 2012.

[9] L. K. Norford and S. B. Leeb, "Non-intrusive electrical load monitoring in commercial buildings based on steady-state and transient load-detection algorithms," *Energy Build.*, vol. 24, no. 1, pp. 51–64, Jan. 1996.

[10] S. R. Shaw and C. R. Laughman, "A Kalman-filter spectral envelope preprocessor," *IEEE Trans. Instrum. Meas.*, vol. 56, no. 5, pp. 2010–2017, Oct. 2007.

[11] S. R. Shaw, S. B. Leeb, L. K. Norford, and R. W. Cox, "Nonintrusive load monitoring and diagnostics in power systems," *IEEE Trans. Instrum. Meas.*, vol. 57, no. 7, pp. 1445–1454, Jul. 2008.

[12] M. L. Marceau and R. Zmeureanu, "Nonintrusive load disaggregation computer program to estimate the energy consumption of major end users in residential buildings," *Energy Convers. Manage.*, vol. 41, no. 13, pp. 1389–1403, Sep. 2000.

[13] L. Farinaccio and R. Zmeureanu, "Using a pattern recognition approach to disaggregate the total electricity consumption in a house into the major end-uses," *Energy Build.*, vol. 30, no. 3, pp. 245–259, Aug. 1999.

[14] M. Baranski and J. Voss, "Genetic algorithm for pattern detection in NIALM systems," in *Proc. IEEE Syst., Man Cybern., Conf.*, 2004, pp. 3462–3468.

[15] D. Srinivasan, W. S. Ng, and A. C. Liew, "Neural-network-based signature recognition for harmonic source identification," *IEEE Trans. Power Del.*, vol. 21, no. 1, pp. 398–405, Jan. 2006.

[16] C. N. Hsu, H. J. Huang, and D. Schuschel, "The ANNIGMA-wrapper approach to fast feature selection for neural nets," *IEEE Trans. Syst., Man, Cybern. B, Cybern.*, vol. 32, no. 2, pp. 207–212, Apr. 2002.

[17] N. Kwak and C. H. Choi, "Input feature selection for classification problems," *IEEE Trans. Neural Netw.*, vol. 13, no. 1, pp. 143–159, Jan. 2002.

[18] M. Kudo and J. Sklansky, "Comparison of algorithms that select features for pattern classifiers," *Pattern Recognit.*, vol. 33, no. 1, pp. 25–41, Jan. 2000.

[19] L. Liu, S. Yang, and D. Wang, "Particle swarm optimization with composite particles in dynamic environments," *IEEE Trans. Syst., Man, Cybern. B, Cybern.*, vol. 40, no. 6, pp. 1634–1648, Dec. 2010.

[20] B. I. Kazem and N. F. H. Zangana, "A neural network based real time controller for turning process," *Jordan J. Mech. Ind. Eng.*, vol. 1, no. 1, pp. 43–55, Sep. 2007.

[21] J. Kennedy and R. Eberhart, "Particle swarm optimization," in *Proc. IEEE Int. Conf. Neural Netw. IV*, 1995, pp. 1942–1948.

[22] Y. Y. Hong and B. Y. Chen, "Locating switched capacitor using wavelet transform and hybrid principal component analysis network," *IEEE Trans. Power Del.*, vol. 22, no. 2, pp. 1145–1152, Apr. 2007.


**Hsueh-Hsien Chang** (S'05–M'05) was born in Taoyuan, Taiwan, in 1966. He received the B.S. and M.S. degrees in electrical engineering from National Taiwan University of Science and Technology, Taipei, Taiwan, in 1994 and 1996, respectively, and the Ph.D. degree in electrical engineering from Chung Yuan Christian University, Jhongli, Taiwan, in 2009.

From 1996 to 1998, he was a Project and System Engineer with ABB Ltd., Taipei. Since 2009, he has been an Assistant Professor with the Department of Electronic Engineering, Jinwen University of Science and Technology, New Taipei, Taiwan. His current research interests include neural networks, evolutionary computing applications in power and energy systems, and power quality of power systems.

Dr. Chang is a member of the IEEE Power Engineering Society, IEEE Industry Applications Society, Institution of Engineering and Technology, U.K., and Taiwanese Association for Consumer Electronics.

**Lung-Shu Lin** received the B.S. degree in electrical engineering from National Taipei University of Technology, Taipei, Taiwan, in 2010 and the M.S. degree in electrical engineering from National Taiwan University of Science and Technology, Taipei, in 2012.

He is currently a Researcher with Chung-Shan Institute of Science and Technology, Taoyuan, Taiwan. His research interests include energy management, power system engineering, and intelligence algorithm.

**Nanming Chen** was born in Tainan, Taiwan, in 1951. He received the B.S. degree in electrical engineering from National Taiwan University, Taipei, Taiwan, in 1973, the M.S. degree in electrical engineering from Virginia Polytechnic Institute and State University, Blacksburg, VA, USA, in 1977, and the Ph.D. degree in electrical engineering from Purdue University, West Lafayette, IN, USA, in 1980.

Since 1989, he has been a Professor with National Taiwan University of Science and Technology (NTUST), Taipei, and a Chair Professor since 2008. From December 2000 to January 2005, he was the Dean of Research and Development with NTUST. From September 2005 to July 2008, he was the Director of the Advisory Office with the Ministry of Education, Taiwan. From July 2004 to August 2007, he was the Director of the Board of Directors of Taiwan Power Company. His research interests include power systems, control systems, and railway electromechanical systems. Another administrative specialty is vocational and technological education.

**Wei-Jen Lee** (S'85–M'85–SM'97–F'07) received the B.S. and M.S. degrees in electrical engineering from National Taiwan University, Taipei, Taiwan, in 1978 and 1980, respectively, and the Ph.D. degree in electrical engineering from the University of Texas at Arlington, Arlington, TX, USA, in 1985.

Since 1985, he has been with the University of Texas at Arlington, where he is currently a Professor in the Department of Electrical Engineering and the Director of the Energy Systems Research Center. He has been involved in the revision of IEEE Stds. 141, 339, 551, 739, and dot 3000 series development. He is the Vice Chair-Papers of the IEEE Industry Applications Society and the Industrial and Commercial Power Systems Department and an Associate Editor of the IEEE Industry Applications Society and the *International Journal of Power and Energy Systems*. He is the Project Manager of the IEEE/National Fire Protection Association Collaboration on Arc Flash Phenomena Research Project. He has served as the Primary Investigator (PI) or Co-PI of over 90 funded research projects. He has provided onsite training courses for power engineers in Panama, China, Taiwan, Korea, Saudi Arabia, Thailand, and Singapore. He has refereed numerous technical papers for the IEEE Institution of Engineering and Technology, U.K., and other professional organizations. He has published more than 260 papers in journals and conference proceedings. He has been involved in research on utility deregulation, renewable energy, smart grid, microgrid, arc flash and electrical safety, load forecasting, power quality, distribution automation and demand-side management, power systems analysis, online real-time equipment diagnostic and prognostic systems, and microcomputer-based instruments for power system monitoring, measurement, control, and protection.

Dr. Lee is a Registered Professional Engineer in the State of Texas.